Int J Adv Struct Eng (2017) 9:205–217
DOI 10.1007/s40091-017-0165-x

STATE-OF-THE-ART

Innovations in rocking wall-frame systems-theory and development

Mark Grigorian[1] · **Shayan Tavousi**[2]

Received: 25 May 2016 / Accepted: 12 July 2017 / Published online: 22 July 2017

Abstract The need to improve the seismic performance of buildings has brought about innovative systems such as rocking wall-moment frame (RWMF) combinations. The behavior of RWMFs can best be visualized by the moment-frame (MF) restraining the wall in place, and the rigid rocking wall (RRW) providing additional damping and imposing uniform drift along the height of the frame. A novel method of analysis followed by the development of a new lateral resisting system is introduced. The proposed concepts lead to an efficient structural configuration with provisions for self-centering, reparability, performance control, damage tolerance and collapse prevention. Exact, unique, closed form formulae have been provided to assess the collapse prevention and self-centering capabilities of the system. The objective is to provide an informative account of RWMF behavior for preliminary design as well as educational purposes. All formulae have been verified by independent computer analysis. Parametric examples have been provided to verify the validity of the proposed solutions.

Keywords Link beams · Rocking wall-frames · Uniform drift · Collapse prevention · Re-centering · Reparability

✉ Mark Grigorian
markarjan@aol.com

Shayan Tavousi
shayantavousi@gmail.com

[1] Structural Engineers Inc., 111 N. Jackson St., Glendale, CA 91206, USA

[2] International Institute of Earthquake Engineering and Seismology, Tehran, Iran

Introduction

The use of rocking systems with gap opening walls and beams have been studied extensively in recent years. The most outstanding contributions in this field are due to Aslam et al. (1980), Englekirk (2002), Ajrab et al. (2004), Panian et al. (2007), Deierlein et al. (2009), MacRae (2011), Seymour and Laflamme (2011), Chou and Chen (2011), Wada et al. (1992, 2012), Janhunen et al. (2012), Eatherton et al. (2014) and Grigorian et al. (2017). The interested reader in rocking frame innovations is referred to well-documented bibliographies by Hajjar et al. (2013) and Chancellor et al. (2014). The important conclusion drawn from current experience is that rocking can provide improved seismic performance with collapse preventive and re-centering potentials. The current paper focuses on the performance of the RWMFs rather than isolated rocking cores. The utility of any rocking systems, as part of a building structure, depends upon the following viability conditions:

1. The relative stiffnesses of the structure and the rocking system (MacRae et al. 2004);
2. The relative strengths of the two systems (Grigorian and Grigorian 2016).
3. Local seismicity and structural archetype (FEMA 2009).
4. Interactions of the two systems at common interfaces (Garlock et al. 2007; Dowden and Bruneau 2011).
5. The response of the freestanding MF on its own (Grigorian and Grigorian 2015).
6. The fact that RWMFs cited in this article have all passed tests of experimentation as well as time–history analysis (Zibaei and Mokari 2014).

These conditions have been employed to propose a new building archetype that incorporates post-tensioned RRWs,

link beams (LBs), buckling restrained braces (BRBs), and a grade beam restrained moment frame (GBRMF). The most compelling utility of the proposed solution is that it allows RWMFs to be designed as damage tolerant systems or in extreme scenarios as collapse prevented structures. All symbols are defined as they first appear in the text.

Conceptual design philosophies

The analytical model of the proposed system is presented in Fig. 1a. The proposed methodology seeks to develop a futuristic structural configuration that also complies with the requirements of conventional systems (FEMA 2006). The fundamental idea behind the proposed methodology is that seismic structural response is mainly a function of design and detailing rather than analysis (Grigorian and Grigorian 2011). The lateral load profile is asserted rather than expected. Both, strength and stiffness are induced rather than investigated. Stability conditions and failure mechanisms are enforced rather than tested. In addition, collapse prevention and self-centering features are integrated as parts of the drift reduction capabilities. The proposed system tends to achieve the same with less damage and cost-effective repair options. Some of the more significant findings incorporated as basic assumptions or direct analytic input can be summarized as follows:

- The RRW acts like a vertical simply supported beam rather than a fixed base cantilever.
- The axial stiffnesses of the BRBs, activated LBs and the RRW can be replaced by equivalent rotational stiffnesses.
- The RRW suppresses all higher modes of vibration to lower levels than associated with axial deformations of the frame.
- A RRW may be considered as rigid if its maximum elastic drift does not exceed 10% of the allowable drift ratio.
- The RWMF remains a single degree of freedom (SDOF) system throughout the loading history of the structure.
- Drift concentration is either nil or insignificant during all loading stages of the structure.
- Gap opening can happen between any two planes perpendicular to the axis of a member.
- The analysis can be immensely simplified, without loss of generality, by considering the lumped stiffnesses, equilibrium and drift compatibility of adjoining subframes, instead of those of the constituent elements of the system.

These ideas have all been utilized to develop the proposed building system and the corresponding analytical model.

Design-led system development

In design-led system development the structure and its elements are configured to perform as expected rather than tested for compliance with the same requirements. The first step in developing the proposed system is to identify the flaws and weaknesses associated with conventional, fixed base, dual systems and to offer rational alternatives. However, adapting the following design strategies can alleviate most or all such flaws:

- Increasing energy dissipation, through steel tendon stretching (Christopoulos et al. 2002),
- providing wall supported and other types of structural dampers and devices, such as LBs, BRBs, friction devices, etc,
- reducing global stiffness in order to increase natural periods of vibrations (Chancellor et al. 2014),
- making demand capacity ratios of as many members as close to unity as possible,
- controlling mode shapes by allowing the first mode of vibrations to suppress all higher modes,
- enforcing sway type collapse mechanism to prevent soft story failure (Wada et al. 1992),
- reducing drift concentration, thereby improving structural performance (Hamburger et al. 2007),

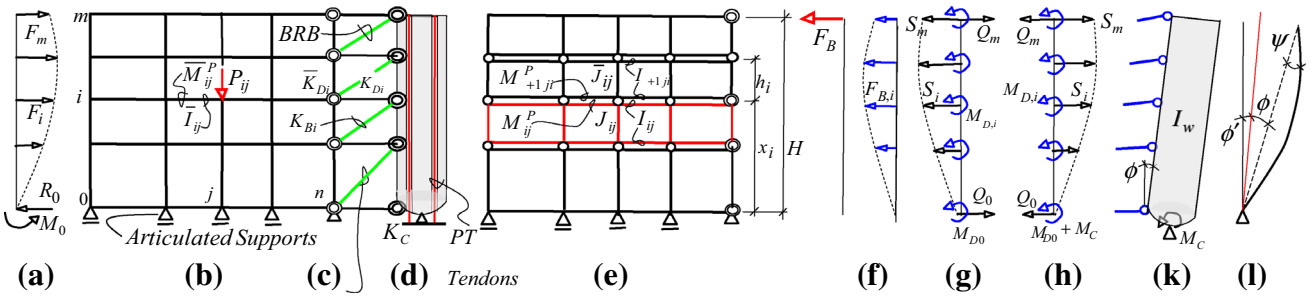

Fig. 1 **a** A lateral loading, **b** grade beam restrained moment frame, **c** link beams, **d** rigid rocking wall, **e** equivalent subframes, **f** buckling restrained brace shear distribution and equivalent forces, **g** link beam forces acting on moment frame, **h** link beam forces acting on rigid rocking wall, **k** rigid wall base moment, **l** rigid wall displacements

- reducing damage by using specific boundary support conditions such as those in GBRMFs,
- designing relatively inexpensive PT cables to remain elastic during earthquakes; and
- increasing repairability, by limiting damage to beams and replaceable items only.

These conditions have been implemented as essential attributes of the RWMF (Fig. 1b–d). In this scheme i and j are the joint coordinates of a $m \times n$ MF. $\bar{I}_{i,j} = I_{i,j} + I_{i+1,j}$ and $\bar{J}_{ij} = J_{ij}$, and $\bar{M}^P_{i,j} = M^P_{i,i} + M^P_{i+1,j}$ and $\bar{N}^P_{i,j} = N^P_{i,j}$ stand for moments of inertias and plastic moments of resistance of beams and columns related to joint ij, respectively. The MF is connected to the RRW by means of pin ended LBs as shown in Figs. 1c and 2a. The rotational stiffness of the RRW (Fig. 1d) is symbolized as K_C. The equivalent rotational stiffnesses of the tendon systems connecting the LBs to the RRW and the MF are given as $K_{D,i}$ and $\bar{K}_{D,i}$, respectively. $K_{B,i}$ is the equivalent rotational stiffness of the BRB at level i. In this paper LBs, BRBs and PT tendons have been used primarily as means of collapse prevention and self-centering rather than damping elements. The mathematical treatment of the proposed structural system is presented in the forthcoming sections.

Potential design advantages

The advantages of implementing the proposed improvements may be summarized as follows:

- The new system is ideally suited for reducing drift and preventing soft story failures in new and existing buildings,
- the new system lends itself well to self-centering, collapse prevention and damage reduction strategies,
- the proposed system attracts substantially less residual stresses and deformations due seismic effects,
- no major anchor bolt, base plate and footing damage can occur due to seismic moments,
- gap openings dissipate seismic energy and provide opportunities for self-centering and collapse prevention,
- RRWs can be used as elements of structural control for pre and post-earthquake conditions,
- the drift profile is not sensitive to minor changes in wall stiffness,
- RWMFs have longer natural periods of vibration than their fixed base counterparts and attract smaller seismic forces,
- RRWs tend to rotate as rigid bodies without significant in or out of-plane deformations,
- RRWs also provide effective protection against near-fault effects at all performance levels,
- the displacement profile remains a function of the same single variable for all loading conditions,
- the structure is a SDOF system, and as such lends itself well to equivalent energy studies,
- the limit state drift ratios are smaller than those of identical frames with fixed and pinned boundary support conditions,
- the magnitude and distribution of P-delta moments are more favorable than in geometrically similar free standing MFs,
- the restraining effects of BRBs can be expressed as notional equivalent overturning moments; and
- RRWs tend to induce points of inflection at mid spans of all beam and columns,
- and the earthquake resisting MFs are designed in accordance with the requirements of the prevailing codes of practice.

Principle design features

The proposed system consists of five essential components; GBRMF, LBs, RRW, BRBs and the stabilizing tendons.

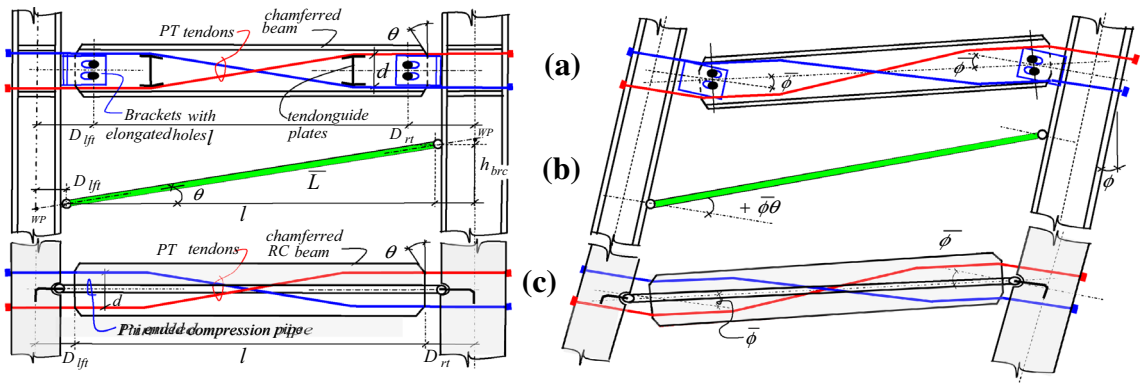

Fig. 2 **a** Chamfered steel LB before and after rotation, **b** BRB before and after rotation, **c** chamfered reinforced concrete LB before and after rotation. (Reinforcing bars and other details not shown for clarity)

- In GBRMFs plastic hinges are forced to form at the ends of the grade beams (not at column supports). The gravity system and the earthquake-resisting MFs are designed in accordance with the requirements of the prevailing codes of practice.
- Conventional PT gap opening systems utilize flat bearing ends. Fully bearing gap-opening devices tend to expand the frame beyond its original span length (Garlock et al. 2007); Dowden and Bruneau 2011). The uncontrolled span expansion induces drift concentration, additional column moments and tends to damage floor level diaphragms. In order to alleviate these effects, a truncated version of the same LB (Fig. 2a, c) has been introduced. The proposed LB consists of a pin ended, steel wide flange beam that contains the PT cables. In order to avoid contact between the column and the truncated ends of the LB, the width of the initial gap should be larger than $\bar{\phi}d/2$.
- The disposition of Post-tensioned (PT) tendons along the wall and the LBs should be in strict conformance with engineering principles. The length, layout, cross-sectional areas, guide plates, the PT forces, etc., should be assessed in terms of the required drift angle, self-centering and collapse prevention requirements. The cable layouts presented in Fig. 2a, b have been devised to reduce loss of stretching due to simultaneous gap opening and closing at both ends of the LB.
- Un-supplemented RRWs neither increase the strength nor the stiffness of the MFs. Seismic shear is transferred to the RWMF through direct shear, PT tendons, LBs, BRBs, as well as shear connectors between the slab and the RRW (Fig. 3a, b). The physical separation between the slab and the wall and the LBs prevents the slab and the wall from being damaged during earthquakes. Figure 3a allows horizontal shear transfer without inhibiting the vertical movement of the wall at the junction. The detail also provides out of plane stability at all floor levels. Figure 3d shows a typical base detail.

BRBs act as axially hysteretic elements. The use of BRBs increases the ductility, strength and stiffness of the RWMF. They can be highly instrumental in implementing drift control, damage reduction and collapse prevention strategies (AISC/SEAOC 2001). The challenge, therefore, is to select the brace force $T_{B.r,i}$, at rth stage loading, for ith level, subframe, in such a way as to reduce the effects of the total external overturning moments including the P-delta and out of straightness, ϕ' effects (Fig. 1l) to more manageable levels. This is achieved by defining an equivalent moment of resistance $M_{B.r}$ and equivalent rotational stiffness $K_{B.r}$ for the braced frame of Fig. 1b. An innovative short cut method for relating $T_{B.r,i}$ to the global drift ratio ϕ_r has been proposed for the specific purposes of the current article.

Theoretical development

The conceptual development presented herein is based on the assumption that the subject MF can be modeled as imaginary subframes stacked on top of each other (Fig. 1e). The RWMF is essentially subjected to two groups of external moments, opposed by as many internal global resisting moments as there are groups of resisting elements. The external overturning moment $M_{0.r}$ is caused by the lateral forces $F_{r,i}$ and the P-delta moment, $M_{P\Delta.r}$. The internal global moments, $M_{F.r}$, $M_{D.r}$, $M_{B.r}$ and $M_{C.r}$, are due to the resistance of the members of the MF, LBs, BRBs and the RRW, respectively, at rth stage loading. The load–displacement relationship of each group of components of each subframe i, such as $M_{F.r,i}$, is derived separately. All subframe moments are then superimposed to establish the global force displacement relationship of the system. The analytic effort leading to the derivation of the characteristic equation of the subject RWMF consists of two independent but interrelated parts. Part one deals with the formulation of the elastic–plastic response of the system to all global moments. Part two discusses the plastic response of the MF at incipient failure (Fig. 4b).

Elasto-plastic response

The purpose of this section was to develop a closed form formula for the response of the imaginary subframe throughout the loading history of the RWMF, starting from

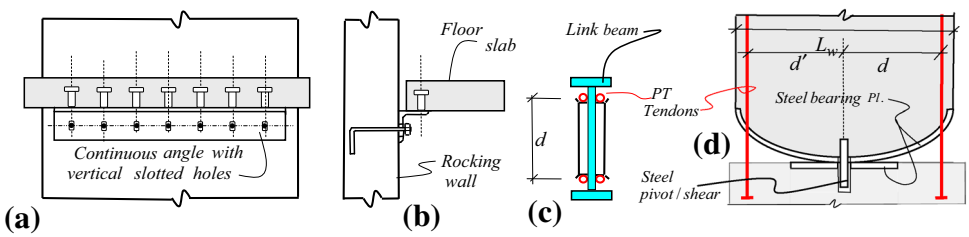

Fig. 3 **a**, **b** Conceptual wall-slab shear connection, **c** link beam section, **d** rocking wall base and cables

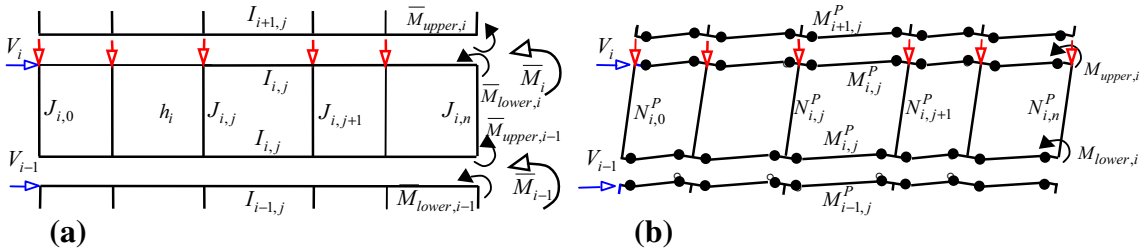

Fig. 4 **a** Subframe under racking shear and LB moments, **b** subframe plastic failure mechanism

zero to first yield, from first yield to incipient frame failure, from frame failure to LB and BRB incapacitation and eventually the collapse of the structure due to wall and/or tendon failure. This could in turn be used to relate collapse prevention, life safety, immediate occupancy and other performance levels to Maximum Considered Earthquake ground motion intensity, Design Basis earthquake and other stipulated criteria (ASCE 2007). The following theoretical strategies have been implemented to reduce the task of otherwise complicated indeterminate analysis to manually manageable static solutions, that

- instead of modeling the axial restraining effects of the LBs, BRBs and the RRW tendons, equivalent rotational schemes have been utilized to capture the restoring effects of these devices against external forces.
- The additional stiffness of a horizontal subframe containing a BRB can be expressed as that of an equivalent pin-jointed subframe with modified properties (Fig. 5) and that,
- The redistribution of moments through formation of plastic hinges at beam ends (Fig. 4b) due to sway type failure forces the points of inflection towards mid spans.

Subframe response due to story level shear

The use of these observations leads to accurate solutions with insignificant margins of error. This can be attributed to the imposition of uniform drift by the RRW and the spread of plasticity over the entire structure. The solution becomes exact at incipient collapse. Since the drift angles $\phi_{r,i} = \phi_r$ and initial imperfection or out of straightness, ϕ' (Fig. 1l) are the same for all subframes i at rth stage loading, then the drift increment equation of any subframe, as in Fig. 1e in terms of story level racking, $M_{0,r,i} = V_{r,i}h_i$ and P-delta moments, $M_{P\Delta,r,i} = (\phi_r + \phi')h_i \sum_i^m \sum_{j=0}^n P_{i,j}$ and subframe stiffness $K_{r,i}$ can be expressed (Grigorian and Grigorian 2012) as follows:

$$\phi_{r,i} = \frac{(V_{r,i}h_i + M_{P\Delta,r.i})}{12E}\left[\frac{1}{\sum_{j=0}^n \bar{\delta}_{i,j}k_{\text{col},i,j}} + \frac{1}{2\sum_{i=1}^n \delta_{i,j}k_{\text{beam},i,j}}\right] = \frac{(M_{0,r,i} + M_{P\Delta,r,i})}{K_{r,i}h_i^2}, \quad (1)$$

where E is the modulus of elasticity, $k_{\text{col},i,j} = J_{i,j}/h_i$ and $k_{\text{beam},i,j} = I_{i,j}/L_j$ are relative stiffnesses. By definition, $P_{i,j}$ and $P_i = \sum_i^m \sum_{j=0}^n P_{i,j}$ are nodal and total accumulative gravity loads acting on level i, respectively. The Kronecker's deltas $\delta_{i,j}^P$ and $\bar{\delta}_{i,j}$ have been introduced to help track the response of the structure as a continuum, they refer to the effects of formation or lack of formation of plastic hinges at the ends of beams i, j. For instance, $\delta_{m,j}^P = 1$ if $M_{i,j} < M_{i,j}^P$ and $\delta_{i,j}^P = 0$, if $M_{i,j} = M_{i,j}^P$. $\delta_{i,j}^P = 0$, also implies structural damage or loss of stiffness with respect to member i,j. $\bar{\delta}_{i,j}$ has been introduced to include the contribution or lack there of column stiffness to overall stiffness $K_{r,i}$ due to the formation of plastic hinges at the ends of the adjoining beams. $\bar{\delta}_{i,j} = 0$ if $M_{i,j} = M_{i,j}^P$ and $M_{i,j-1} = M_{i,j-1}^P$; otherwise $\bar{\delta}_{i,j} = 1$. M^P stands for plastic moment of resistance. Next, bearing in mind that the sum of story level overturning moments, $(V_{r,i}h_i + M_{P\Delta,r,i})$ is equal to the total external overturning moment $(M_{0,r} + M_{P\Delta,r})$ what gives

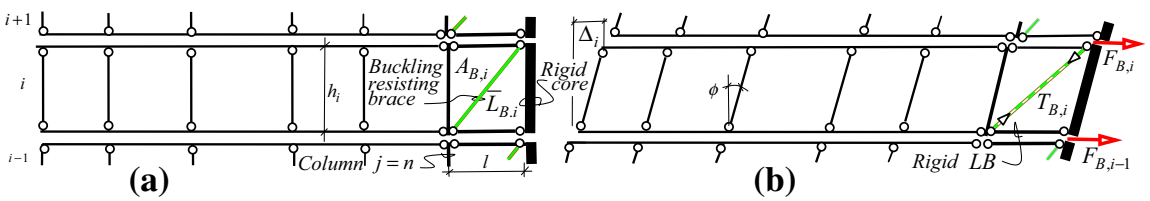

Fig. 5 **a** Subframe i and BRB before rotation, **b** subframe i and BRB after rotation

$$M_{0,r} + M_{P\Delta,r} = \sum_{i=1}^{m} \left(V_{r,i}h_i + M_{P\Delta.r,i}\right) = \sum_{i=1}^{m} \phi_{r,i}K_{r,i}h_i^2 \text{ or } \phi_r = \frac{M_{0,r} + M_{P\Delta,r}}{\sum_{i=1}^{m} K_{r,i}h_i^2}. \quad (2)$$

The denominator of Eq. (2) represents the rotational stiffness of the un-supplemented RWMF under lateral and *P*-delta effects. It represents a closed form solution that can estimate lateral displacements and member forces of RWMFs throughout the entire linear and nonlinear static ranges of loading. In Eq. (2) shear, panel zone, hinge offset, axial load and other secondary effects have been discarded in favor of simplicity. Equation (2) is highly versatile in that it contains all plausible performance levels that affect structural response, safety and property protection. The contributions of supplementary LBs, BRBs and the post-tensioned RRW are discussed in the few sections.

Development of subframe and LB load–displacement relationship

Since any two vertically stacked subframes share the same LB, it would be rational to divide the gap opening moment $\bar{M}_i = T_{L,i}d_i/2$ in proportion to their stiffnesses, i.e., $\bar{M}_{\text{upper},i} = I_{i+1}\bar{M}_i/(I_i + I_{i+1})$ and $\bar{M}_{\text{lower},i} = I_i\bar{M}_i/(I_i + I_{i+1})$, where $T_{L.r,i} = T_{L.r}$ is the LB tensile force (Fig. 2a, b). Since both the wall and the column are assumed to be locally rigid, the magnitude of the gap rotation $\bar{\phi}$ can be expressed as a function of the LB length l and the adjoining wall and column offset distances D_{lft} and D_{rt}, respectively (Fig. 2a, i.e).

$$\bar{\phi} = \left[\frac{D_{\text{lft}} + D_{\text{rt}} + 2l}{2l}\right]\phi = \alpha\phi \quad (3)$$

Smaller $\bar{\phi}$ implies smaller gap opening force than that experienced by the link assembly. The relationship between the wall side gap opening and the corresponding tendon extension at any loading stage r may be expressed as follows:

$$\bar{\phi}_{r,i} = \alpha\phi_{r,i} = \frac{2T_{L.r,i}L_L}{dA_LE_L} = \frac{4T_{L.r,i}dL_{Lb}}{2d^2A_LE_L} = \frac{M_{D.r,i}}{K_D} \quad \text{and} \quad K_D = \frac{d^2A_LE_L}{4L_L}. \quad (4)$$

Let E, A and L represent modulus of elasticity, cross-sectional area and length, respectively. Suffixes L, B and W refer to link beams, braces and wall tendons, respectively. The frame side column is not rigid. The drift reduction on a subframe due to opposing moments $\bar{M}$, (Fig. 4a) can be computed as

$$\varphi_{r,i} = \frac{(\bar{M}_{r,\text{lower},i} + \bar{M}_{r,\text{upper}.i-1})}{24E}\left[\frac{1}{\sum_{j=1}^{n}\delta_{i,j}k_{\text{beam}.i,j}}\right]. \quad (5)$$

However, for $I_i = I$ and $K_{D,i} = K_D$, $\bar{M}_{\text{upper},i-1} = \bar{M}_{\text{lower},i} = \bar{M}_i/2 = \bar{M} = T_fd/4$. Equation (5) reduces to

$$\varphi_{r,i} = \frac{\bar{M}_{r,i}}{12E}\left[\frac{1}{\sum_{j=1}^{n}\delta_{i,j}k_{\text{beam}.i,j}}\right] = \frac{\bar{M}_{r,i}}{\bar{K}_{r,i}} = \frac{(\alpha K_D\phi_{r,i})}{\bar{K}_{r,i}} = \bar{K}_{D.r,i}\phi_{r,i}. \quad (6)$$

If there is $m - s$ number of active LBs above level s, where, $0 \geq s \geq m$, then the total restoring moment of all activated subframes, $M_{D,r}$ can be computed as

$$M_{D,r} = \sum_{i=s}^{m}\bar{M}_{r,i} = \sum_{i=s}^{m}\phi_{r,i}\bar{K}_{r,i} \text{ or } \phi_r = \frac{\sum_{i=s}^{m}\bar{M}_{r,i}}{\sum_{i=s}^{m}\bar{K}_{r,i}} = \frac{\alpha(m-s)K_D\phi_{r,i}}{\sum_{i=s}^{m}\bar{K}_{r,i}}. \quad (7)$$

The net effect of the overturning and opposing moments on the MF can be computed as

$$\phi_r = \frac{(M_{r,0} + M_{P\Delta,r})}{K_{F,r}} - \varphi_r = \frac{(M_{r,0} + M_{P\Delta,r})}{K_{F,r}} - \bar{K}_{D,r}\phi_r \quad \text{or} \quad \phi_r = \frac{(M_{r,0} + M_{P\Delta,r})}{(1 + \bar{K}_{D,r})K_{F.r}}, \quad (8)$$

where $\bar{K}_{D.r} = \alpha(m-s)K_D/\sum_{i=s}^{m}\bar{K}_{r,i}$ and $(1 + \bar{K}_{D.r,i})K_{F.r}$ are the contributions of the frame side LBs and the equivalent stiffness of the subframe, respectively. It is instructive to note that as plastic hinges form at the ends of the beams of the subframe, the relative stiffness EI/L of all beams become zero. And, if all active LBs can develop their ultimate moments of resistance $M_{D,i}^P = \bar{M}_{\text{upper},i}^P + \bar{M}_{\text{lower},i+1}^P$, then the ultimate carrying capacity of the MF, including the LBs becomes

$$(M_0^P + M_{P\Delta}^P) = 2\sum_{i=s}^{m}M_{D,i}^P + 2\sum_{j=1}^{n}\sum_{i=0}^{m}\bar{M}_{i,j}^P. \quad (9)$$

As I_i tend toward zero, the rotational springs prevent subframe collapse, and Eq. (8) reduces to

$$\phi_P = \frac{M_0^P + M_{P\Delta}^P}{\alpha(m-s)K_D}. \quad (10)$$

Development of subframe and BRB load–displacement relationship

Consider the displacements of the imaginary braced frame of Fig. 1, composed of the end column at $j = n$ and the RRW as its vertical chords, and LBs and BRBs as its

horizontal and diagonal elements, respectively. The RRW imposes a straight drift profile on the MF and the braced frame. As a result, each subframe, such as that shown in Fig. 5b, displaces an amount $\Delta_{r,i} = \phi_r h_i$, with respect to its lower chord. The challenge here is to relate the brace force $T_{B.r,i}$ to the drift ratio ϕ_r.

This is achieved by assuming all members of the MF are axially rigid and constitute an unstable mechanism (Fig. 5a). The axial deformation Δ_i of any such brace can be related to the uniform drift ratio, i.e.,

$$\Delta_{r,i} = \frac{\alpha\phi_r h_i l}{\bar{L}_{B.i}} = \frac{T_{B.r,i}\bar{L}_B}{A_{B.i}E_B},\ T_{B.r,i} = \frac{\alpha\phi_r h_i l A_{B,i}E_B}{\bar{L}^2_{B.i}} \quad \text{or} \quad A_{B,i} = \frac{T_{B.r,i}\bar{L}^2_{B.i}}{\alpha\phi_r h_i l E_B}. \tag{11}$$

Let $F_{B.r,i}$ stand for the equivalent notional lateral load corresponding to BRB force $T_{B.r,i}$ of Fig. 5b. Next, consider the compatible rigid body rotations, $\phi_{B.r}$ of all subframes. If there is $m - u$ number of BRBs above level u, $0 \geq u \geq m$, then the corresponding virtual work equation can be written down as

$$\sum_{i=u}^{m} F_{B.r,i}\phi_r x_i = \phi_r M_{B,r} = \sum_{i=u}^{m} T_{B.r,i} \qquad \Delta_{r,i} = \sum_{i=u}^{m}\left[\frac{\alpha^2\phi_r^2 h_i^2 l^2 A_{B,i}E_B}{\bar{L}^3_{B.i}}\right], \tag{12}$$

or

$$\phi_{B,r} = \frac{M_{B,r}}{\alpha^2 l^2 E_B \sum_{i=u}^{m}(h_i^2 A_{B,i}/\bar{L}^3_{B.i})} = \frac{M_{B,r}}{K_{B,r}}. \tag{13}$$

This implies that the braced frame tends to oppose the external overturning moment by a notional global moment of resistance related to the axial resistance of the BRBs. Following Eq. (8), it gives

$$\phi_r = \frac{(M_{0,r} + M_{P\Delta.r}) - M_{B,r}}{(1 + \bar{K}_{D,r})K_{F,r}}, \quad \text{or} \quad \phi_r = \frac{(M_{0,r} + M_{P\Delta.r})}{K_{B,r} + (1 + \bar{K}_{D,r})K_{F,r}}. \tag{14}$$

However, it is computationally expedient to deal with a single force $F_{B,m} = T_m l/\bar{L}_m$ as shown in Fig. 1f rather than the generalized distribution of forces $F_{B,i}$ of the same figure that result in a stepwise variation of shear forces along the frame. The brace force distribution due to the former strategy can be expressed as $T_m = F_{B,m}\bar{L}_m/l, \ldots,$ $T_i = F_{B,m}\bar{L}_i/l, \ldots,$ and $T_1 = F_{B,m}\bar{L}_1/l$. This allows all brace sectional areas $A_{B,i}$ to be related to any known value such as $A_{B,m}$, i.e., $A_{B,i} = (\bar{L}_i/\bar{L}_m)^3(h_m/h_i)A_{B,m}$. Since all brace forces are functions of the same variable ϕ and that internal forces of all members are in static equilibrium, the global moment due to brace resistance can be directly assessed as $M_B = T_m l H/\bar{L}_m$. If M_B reaches its ultimate value, then the total carrying capacity of the system can be estimated as

$$\sum_{i=1}^{m} F^P_{B,i}x_i = M^P_B = \sum_{i=1}^{m} T_{ult,i}\frac{\alpha h_i l}{\bar{L}_{B.i}} \tag{15}$$

If ϕ exceeds $\phi_{\text{Rqd.}}$, or $K_{F,r}$ is deemed inadequate, then Eq. (15) may be utilized to assess the additional stiffnesses of the BRBs required to satisfy the prescribed requirements:

$$K_{B.r} = \frac{(M_{0,r} + M_{P\Delta,r}) - \phi_r(1 + \bar{K}_{D.r})K_{F,r}}{\phi_r}. \tag{16}$$

Development of MF and RRW displacement relationship

The function of the unbonded, tendons (Figs. 1d, 3d) is to stabilize and add strength and stiffness to the RRW. The pair of parallel tendons and the pivot at the base constitutes a rotational spring of stiffness, K_C, designed to remain elastic during and after an earthquake. Therefore, the stress–strain relationship of the wall base spring at any loading stage, r, can be expressed as a linear function of $\phi_r = M_{C,r}/K_{C,r}$, - where $M_{C,r}$ represents the moment of resistance of the spring due to ϕ_r, i.e., $\phi_r d' = \varepsilon_{W.r}L_W$. Substitution of $\varepsilon_{W.r} = T_{W.r}/A_W E_W$ and $M_{C,r} = T_{W,r}d'$ in the strain equation gives $K_{C,r} = d'^2 A_W E_W/L_W$ Following Eq. (14), the contribution of K_C to the response of the RWMF can be examined as

$$\phi_r = \frac{(M_{0,r} + M_{P\Delta.r}) - M_{C,r}}{K_{B.r} + (1 + \bar{K}_{D.r})K_{F.r}} \quad \text{or} \quad \phi_r = \frac{(M_{0,r} + M_{P\Delta.r})}{K_{C.r} + K_{B.r} + (1 + \bar{K}_{D.r})K_{F.r}} = \frac{(M_{0,r} + M_{P\Delta.r})}{K^*_r}. \tag{17}$$

Equation (17) is the most generalized characteristic load–displacement equation of the RWMF, where K^*_r represents the global stiffness of the system at any loading stage, r. K^*_r contains a continuum of ten distinct and several intermediate levels of response: $r = 0$ (at rest), $r = E$ (elastic MF, before first yield), $r = Y$ (MF at first yield), $r = C$ (MF at incipient collapse), $r = B_E$ (at BRB elastic level), $r = B_Y$ (BRB at first yield), $r = L_E$ (at LB elastic level), $r = L_Y$ (LB at first yield), $r = C_E$ (wall cables at elastic level), $r = C_Y$ (wall cables at first yield) or $r = W$ (at wall failure) Intermediate levels can be defined in terms of fractions of stages of r, e.g., $r = 0.6$ yield (60% first yield) or $r = 0.3$, device (30% device failure), etc.

Effects of initial imperfections and *P*-delta moments

GBRMFs and RRWs are inherently more prone to initial out of straightness and *P*-delta effects than their fixed base

counterparts. Initial imperfections can occur due to a number of reasons, including construction inaccuracies, foundation failure, shrinkage, residual displacements, etc. However, noting that $M_{P\Delta,r} = \sum_{i=1}^{m}\sum_{j=0}^{n} P_{i,j}(\phi_r + \phi')x_i = (\phi_r + \phi')P^*\bar{H}$, Eq. (17) can also be re-written in the more familiar form:

$$\phi_r = \frac{M_{0.r} + \bar{M}_{0.}}{f_{Cr,r}[K_{C.r} + K_{B.r} + (1 + \bar{K}_{D.r})K_{F.r}]} = \frac{M_{0,r} + \bar{M}_0}{f^*_{CR.,r}K^*_r} \quad \text{and} \quad \bar{M}_0 = P^*\bar{H}\bar{\phi}. \tag{18}$$

$f^*_{Cr.r} = [1 - P^*\bar{H}/K^*_r]$ is the global load reduction factor due to destabilizing effects of $P^* = \sum_{i=1}^{m}\sum_{j=0}^{n} P_{i,j}$ acting at the center of gravity of P^* at $\bar{H}$. Finally, if a state of damage-tolerant design is specified, then Eq. (18) would have to be amended by replacing $(M_{0.r} + \bar{M}_0)$ and $(1 + \bar{K}_{D.r})K_{F.r}$, with $(M^P_0 + M^P_{P\Delta})$ and $\alpha(m - s)K_D$, respectively.

Nonlinear static analyses

While nonlinear dynamic analysis is known to provide realistic models of structural response to seismic events, nonlinear static procedures can also provide reliable means of design for structures whose dynamic behavior is governed by highly dominant first-mode sway motions (Deierlien et al. 2010). RWMFs being SDOF systems are ideally suited for nonlinear static modeling. FEMA (2005) provides guidelines on the simplifying assumptions and limitations on nonlinear static seismic analysis procedures. The mathematical model described by Eqs. (17) and (18) contains the entire spectrum of nonlinear static responses and satisfies all conditions of the uniqueness theorem; therefore, it cannot be far from a minimum weight solution. Assuming that plastic moments of resistance of the beams and supplementary devices are given by $\bar{M}^P_{i,j}$, $M^P_{D,i}$, $M^P_{B,i}$ and M^P_C, respectively then the ultimate carrying capacity of the entire system can be estimated as

$$(M^P_0 + M^P_{P\Delta}) = M^P_C + 2\sum_{i=s}^{m} M^P_{D.i} + \sum_{i=u}^{m} M^P_{B,i} + 2\sum_{j=1}^{n}\sum_{i=0}^{m} \bar{M}^P_{i,j}. \tag{19}$$

Once again, if a state of damage tolerant design is specified, then the last term in Eq. (19) would have to be replaced with its elastic counterpart, $2\sum_{j=1}^{n}\sum_{i=0}^{m}\bar{M}_{i,j}$. Equation (19) can also be used to establish the load factor needed to assure collapse prevention and self-centering, in which case it would be appropriate to assume; $M^P_C > 2\sum_{i=0}^{m} M^P_{D,i} > M^P_B > 2\sum_{j=1}^{n}\sum_{i=1}^{m}\bar{M}^P_{i,j}$. Equation (19) allows the following four distinct plastic failure scenarios to be envisaged.

RWMF with no supplementary devices, $M^P_C = M^P_D = M^P_B = 0$

The LBs do not provide rotational stiffness and transmit only axial forces. The frame is designed to fail in a purely sway mode as in Fig. 6d. The corresponding carrying capacity can be related to the sum of the ultimate resistances of the subframes as;

$$(M^P_0 + M^P_{P\Delta}) = 2\sum_{j=1}^{n}\sum_{i=0}^{m}\bar{M}^P_{i,j}. \tag{20}$$

Note that the RRW, being a mechanism, cannot improve the ultimate carrying capacity of a device free MF. Substitution of $K_F = K_C = K_D = K_B = 0$, into Eq. (17) will lead to the corresponding drift ratio described by Eq. (10) above.

RWMF with no wall-mounted supplementary devices, $M^P_D = M^P_B = 0$ and $M^P_C \neq 0$.

As in the previous case, the LBs transmit axial forces only. In this case the frame will also fail in a purely sway

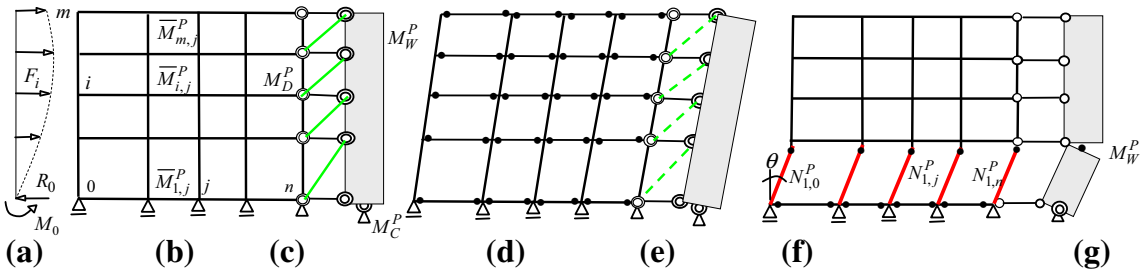

Fig. 6 **a** Loading, **b** proposed dual system, **c** RRW, **d** MF failure, **e** BRB failure, **f** soft story failure of MF and **g** soft story failure of RRW. It should be noted that well-proportioned moment frames of RWMF are designed to fail in a purely sway mode as opposed to involving a beam or combined beam-sway mechanism. The small load theorem for earthquake resisting moment frames (Grigorian and Grigorian 2012), provides limiting magnitudes for gravity loads below which no beam type failure mechanism can take place

mode, with the wall tendons either remaining elastic or yielding in tension. The corresponding collapse load can be estimated as

$$(M_0^P + M_{P\Delta}^P) = M_C^P + 2\sum_{j=1}^{n}\sum_{i=0}^{m}\bar{M}_{i,j}^P. \quad (21)$$

The corresponding drift ratio can now be estimated by inserting $K_F = K_D = K_B = 0$ in Eq. (17). In conclusion, a properly designed rocking wall can actually prevent plastic collapse of the entire system.

Fully supplemented RWMF with no wall tendons $M_C^P = 0$, $M_D^P \neq 0$ and $M_B^P \neq 0$.

In this particular case the MF will also fail in a purely sway mode, with the LB tendons remaining elastic or yielding in tension. The corresponding collapse load can be computed as

$$(M_0^P + M_{P\Delta}^P) = 2\sum_{i=s}^{m} M_{D,i}^P + 2\sum_{j=1}^{n}\sum_{i=0}^{m}\bar{M}_{i,j}^P + \sum_{i=u}^{m} M_B^P. \quad (22)$$

Following the arguments leading to Eq. (17), the drift ratio can now be computed by replacing $K_i h_i^2(1 + \bar{K}_{D,i})$ with $\alpha K_{D,i}$ and inserting $K_C = 0$ in Eq. (17). The post failure static stability of the MF suggests that a well-designed array of LBs and BRBs can either on their own or in conjunction with a properly designed, pre-tensioned RRW help prevent total collapse and re-center the system after a major seismic event. Naturally, collapse prevention can be achieved if a pre-assigned drift ratio can be sustained while safely resisting $\Omega(M_0^P + M_{P\Delta}^P)$, where Ω is the over strength factor defined by the codes.

Determination of wall strength, $K_D = K_B = K_C = 0$

The purpose of the current section was to establish the minimum strength of the wall in such a way as to prevent soft story failure, study its effects on the strength of the frame, compute the lateral displacements at incipient collapse and to show that a well-controlled design can meet both the target drift as well as the prescribed demand-capacity requirements. Since the RRW is a mechanism, it cannot enhance the carrying capacity of its companion frame at collapse, but its own capacity need not be less than the demand imposed upon it by the interactive forces Q_m and S_i shown in Fig. 1g, h. The largest expenditure of energy is generally associated with first level soft story failure, as depicted in Fig. 6f, g. If the plastic moments of resistance of the columns are deliberately selected as $N_{i,j}^P = \lambda(M_{i,j}^P + M_{i,j\text{-}1}^P)$, where $\lambda > 1$ is the column over strength factor, then the virtual work equation for this failure mode can be expressed as $M_0^P\theta + P^* h_1\theta = 2\sum_{j=1}^{n}\bar{M}_{1,j}^P\theta + \sum_{j=0}^{n} N_{1,j}^P\theta + M_w^P\theta$ which yields the wall strength as

$$M_w^P > 2\sum_{j=1}^{n}\bar{M}_{1,j}^P + \sum_{j=0}^{n} N_{1,j}^P - (M_0^P + P^* h_1). \quad (23)$$

With M_0^P known, the value of M_w^P can be extracted from Eq. (23). The use of Eq. (23) is demonstrated in "Appendix 1".

RWMF design strategies

A wide range of design strategies, depending on the nature of the interactive forces S_i, can be envisaged. Forces S_i are needed to design the elements of the LBs and the RRW. The superposition of results of the preceding sections leads to the expanded version of the characteristic equation of bending of subframe i at response stage r, i.e.,

$$(V_{r,i}h_i + M_{P\Delta.r,i}) = \phi_r[K_{C.r,i} + K_{B.r,i} + (1 + \bar{K}_{D.r,i})K_{F.r,i}] = \phi_r K_{r,i}^*. \quad (24)$$

Consider the combined effects of the external forces F_i and reactive forces Q_m and S_i of Fig. 1g and h on the subject MF; then for $i = m$, and $V_m = F_m + Q_m - S_m$, Eq. (24) gives

$$V_{r,m} = F_{r,m} + Q_{r,m} - S_{r,m} = \phi_r[K_{r,m}^*/h_m - P_m]. \quad (25)$$

Application of Eq. (25) for $i = m - 1$ yields

$$\begin{aligned} V_{r,m-1} &= F_{r,m} + F_{r,m-1} + Q_{r,m} - S_{r,m} - S_{r,m-1} \\ &= \phi_r[K_{r,m-1}^*/h_{m-1} - P_{m-1}]. \end{aligned} \quad (26)$$

Subtracting (25) from (26) and rearranging gives

$$\begin{aligned} V_{r.m-1} - V_{r,m} &= F_{r,m-1} - S_{r,m-1} \\ &= \phi_r[(K_{r,m-1}^*/h_{m-1}) - (K_{r,m}^*/h_m) - (P_{m-1} - P_m)]. \end{aligned} \quad (27)$$

It follows, therefore, that with ϕ_r available from Eq. (17), $S_{i,r}$ can be computed as

$$S_{r,i} = F_{r,i} - \phi_r[(K_{r,i}^*/h_i) - (K_{r,i+1}^*/h_{i+1}) - (P_i - P_{i+1})]. \quad (28)$$

While Eq. (28) contains a large number of solutions, two extreme but important scenarios come to mind, $S_i = 0_i$ and $S_i = F_i$. The two limiting cases describe the use of RWMF combinations as either counterproductive, or highly efficient. These limiting cases are known as MFs of uniform sections or uniform shear (MFUS) and MFs of uniform response (MFUR), respectively. The attributes of both cases are briefly discussed in the next two sections.

Case 1, $S_{r,i} = 0$, attributes of MFUR

The first case implies no wall-frame interaction, i.e., either $E_w I_w = 0$ or the free standing MF is an MFUR (Fig. 7a). In MFUR, groups of members such as beams and columns respond identically to external forces. Elements of the same

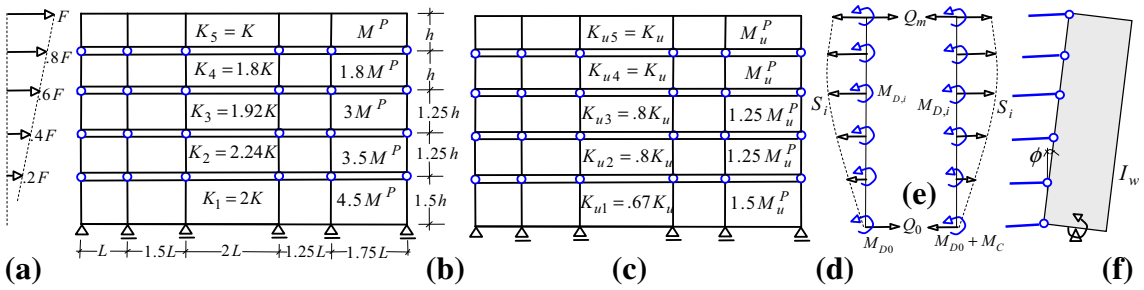

Fig. 7 **a** Loading, **b** MFUR subframe stiffnesses and beam plastic moments, **c** MFUS subframe stiffnesses and beam plastic moments, **d** interactive forces acting against the MF and **e** Interactive forces acting against the RRW

group are designed to simultaneously undergo identical deformations and to develop equal stresses throughout the structure (Grigorian and Grigorian 2011). MFUR act as frameworks of equal strength and stiffness in which members of the same group share the same demand-capacity ratios regardless of their location within the system. Substituting $S_{r,i} = 0$ and $F_{r,i} = V_{r,i} - V_{r,i+1}$ in Eq. (28) gives

$$F_{r,i} = \phi_r[(K^*_{r,i}/h_i) - (K^*_{r,i+1}/h_{i+1}) - P_i]. \tag{29}$$

Since ϕ_r is constant for all i, then Eqs. (25) and (26) lead to the interpretation that

$$\phi_r = \frac{V_{r,m}h_m}{K^*_{r,m} - P_m h_m} = \frac{V_{r,i}h_i}{K^*_{r,i} - P_i h_i}. \tag{30}$$

In MFUR the demand-capacity ratios for groups of elements such as beams, columns, connections, etc., remain constant during all phases of loading, and as such

$$M_i^P = \left(\frac{V_i}{V_m}\right)\left(\frac{h_i}{h_m}\right)\left(\frac{1 - P_m/K_m h_m}{1 - P_i/K_i h_i}\right)M_m^P. \tag{31}$$

MFUR are highly optimized systems that can be used to assess the efficiencies of geometrically identical structures under similar loading and boundary conditions. Since $\phi_i = \phi$ and the frame obeys the rules of proportionality, it can no longer benefit fully from the stiffness of the wall. The obvious conclusion drawn here is that it would be counterproductive to use RRWs in conjunction with MFUR. The attributes of a typical MFUR are briefly illustrated in "Appendix 2".

Case 2 $S_i = F_i$, attributes of MFUS

MFUS can also be categorized as MFUR except that members of the same group of elements possess the same section properties, regardless of their location within the MF. The use of RRWs in conjunction with MFUS can be highly effective in improving the lateral resistance of otherwise poorly performing MFUS. The second scenario, $S_i = F_i$, implies that the wall is rigid, and absorbs the entire external load, and that the MF obeys the rules of Eq. (27), i.e.

$$V_{r,i} - V_{r,i+1} = \phi_r[(K^*_{r,i}/h_i) - (K^*_{r,i+1}/h_{i+1}) - (P_i - P_{i+1})] = 0. \tag{32}$$

In other words both $\phi_{r,i} = \phi_r$ and $V_{r,i} = V_r$ are constant for the same r along the height of the structure, or

$$\phi_r = \frac{V_{r,m}h_m}{K^*_{r,m} - P_m h_m} = \frac{V_{r,i}h_i}{K^*_{r,i} - P_i h_i}. \tag{33}$$

Since $S_i = F_i$ then the generalized rocking wall equilibrium equation may be rewritten as

$$Q_{r,m}H + [K_{C.r} + (m - s)K_{D.r} - (M_{0,r} + M_{P\Delta.r}) = 0. \tag{34}$$

The free body diagrams of the subframes and the rocking wall of the subject RWMF are shown in Fig. 7c through f. The resulting frame as depicted in Fig. 7c is known as an MFUS. While the use of free standing MFUS may appear counterintuitive, their combination with properly designed RRWs can lead to the development of highly efficient RWMFs. An even more counterintuitive but highly efficient condition arises when $h_i = h$. For equal or nearly equal story heights, $K_{u,i} = K_u$, i.e., $I_{i,j} = I$, implying that all horizontal members can be the same. Similarly, since $J_{i,j} = J$, all columns can also be the same. Example 3 ("Appendix 3") provides a tractable comparison between the performances of an idealized MFUS and a seemingly inefficient MFUS as part of a simple RWMF without supplementary devices.

Determination of wall stiffness

The nature of the interactive forces S_i and Q_m suggests that the wall tends to bend as an upright simply supported beam with a rigid body tilt ϕ. Hence, the conclusion that the stiffer the wall, the better the expected performance of the RWMF. The reactive forces reach their maxima, as the wall becomes stiffer. However, if the rigidity of the wall were to be large but finite and $h_i = h$, then the following design data in the form of maximum wall drift or end slope $\psi_{\max}$ may be found useful for preliminary estimation of

wall stiffnesses under commonly occurring distributions of lateral forces, e.g.,

$$\text{Uniform load}: \ \psi_{\max} = \frac{Fh^2 m(m-1)(m^2+m-2)}{24E_w I_w} \quad \text{and} \quad I_{w,\min} = \frac{Fh^2(m-1)(m^2+m-2)}{24E_w \varepsilon\phi}, \tag{35}$$

$$\text{Triangular}: \ \psi_{\max} = \frac{Fh^2(m-1)(2m-1)(2m^2+3m-4)}{180E_w I_w m} \quad \text{and} \quad I_{w,\min} = \frac{Fh^2(m-1)(2m-1)(2m^2+3m-4)}{180E_w \varepsilon\phi m}. \tag{36}$$

For practical design purposes the stiffness of the wall can be related to a fraction of the prescribed uniform drift say $5\%\phi$ or $\psi_{\max} = \varepsilon\phi$; however, convergence is rapid and results in highly workable initial values.

Collapse prevention and self centering

ASCE (2007) guidelines for the rehabilitation of existing buildings define specific performance levels for immediate occupancy, life safety and collapse prevention, where collapse prevention is defined as "the post earthquake damage state in which the building is on the verge of partial or total collapse". The current section focuses briefly on collapse prevention employing RWMF technologies for both new as-well-as existing structures. Seismic collapse is usually triggered by structural instability or the *P*-delta phenomenon, preceded by the formation of partial or complete ductile failure mechanisms. Plastic failure modes such as those shown in Fig. 6d and f undergo large lateral displacements that in turn lead to catastrophic collapse. While gravity forces, as active components of the *P*-delta effect, are constant quantities, lateral displacements can be controlled even reversed by means of RWMF capabilities suggested by Eqs. (17) or (18), provided that residual effects are small (MacRae and Kawashima 1997), the wall remains elastic and suppresses soft story failure.

The preventive mechanism

The proposed structural system contains three independent drift-restraining mechanisms: the post-tensioned RRW, the LBs and the BRBs. These devices can be utilized either on their own or in combination with each other. The formation of the plastic failure mechanism implies that all K_i are zero, and that as $I_{i,j}$ diminish the limit of $K_{r,i}h_i^2(1+\bar{K}_{D.r,i})$ tend toward. Subsequently, the global stiffness of the combined system reduces to $K^* = K_C + K_B + 2\alpha\sum_{i=0}^{m} K_{D,i}$. In other words if complete collapse is to be prevented after formation of the preferred plastic mechanism, then the surviving LBs, BRBs and the vertical cable system should be strong enough to withstand the entire conditional demand. However, it would be safe to assume that for all practical purposes the PT wall alone is capable of withstanding the earthquake-induced *P*-delta effects, in which case the pertinent global stiffness maybe estimated at $K^* = K_C$. The PT tendons not only act as lateral stabilizers, but also add strength and stiffness to the frame and the wall. Their inherent elasticity helps re-center the structure after an earthquake. The rotational stiffness of the base level cable arrangement has been defined as $K_{C,r} = d'^2 A_W E_W / L_W$. With P^* and ϕ_{collapse} known, the required parameters for collapse prevention can be computed as

$$T_w > \Omega(M_0 + \bar{M}_0)/d' = \Omega(2M_0 + P^*\phi_{\text{collapse}}\bar{H})/2d' \quad \text{and} \quad A_W E_W = T_w H/\phi_{\text{collapse}} d'. \tag{37}$$

Following Eq. (37) the total horizontal tendon force composed of initial tendon force $T_{W.0}$ and that due to additional extensions can be shown to be equal to

$$T_w = T_{W,0} + 2d'\left[\frac{(E_C A_C/H)(E_T A_T/L_T)}{(E_C A_C/H) + E_T A_T/L_T}\right]\phi. \tag{38}$$

Subscripts C and T refer to concrete and tendon, respectively. Here, the wall height, H, and the cable length, L_T, are not necessarily the same. Theoretically speaking, T_W should be sufficiently large to re-center the structure; otherwise, residual deformations under seismic loading can significantly affect the re-centering capacity of the system.

Conclusions

A relatively new seismic structural system that combines BRBs, LBs and RRWs with GBRMFs has been introduced. The seismic behavior of the proposed RWMF can be characterized by the combined responses of the ductile MF and the supplementary devices. In addition to BRBs, both vertical as well as horizontal gap opening devices have been provided to ensure collapse prevention and active re-centering. PT provides restoring forces at the ends of the LBs and the RRW that tend to prevent catastrophic collapse and force the frame and the wall to return to their pre-earthquake positions. The proposed mathematical model lends itself well to SDOF treatment. Several theoretically exact formulae for the preliminary design of regular RWMFs have been presented. The proposed concepts lead to minimum weight solutions. A new gap opening LB that does not induce unwanted moments in the columns and causes no damage to the diaphragms has also been introduced. It has been shown that the magnitude of the LB gap

opening is a function of the link beam offsets from the centerlines of its supporting walls or columns. In the interim two new classes of moment frames, MFUR and MFUS have also been introduced. It has been argued that the use of RRWs in conjunction with MFUR is counter-productive; in contrast the MFUS–RRW combination can lead to highly efficient earthquake-resisting buildings. While the accuracy of the proposed formulae has been verified by independent computer analysis, results may differ due to shear and axial strains, shrinkage and tendon relaxation, etc. The proposed structural scheme is still in its infancy and needs the test of time before being recognized as a viable earthquake-resisting system.

Appendix 1: example 1, minimum wall strength

The utility of Eq. (23) is demonstrated by the following simple example: Let, $F_i = Fi/m$, $P_{i,j} = \phi' = 0$, $\bar{M}^P_{i,j} = \bar{M}^P$, $\bar{M}^P_{0,j} = \bar{M}^P_{m,j} = \bar{M}^P/2$, $N^P_{1,0} = N^P_{1,n} = \lambda\bar{M}^P/2$, $N^P_{i,j} = \lambda\bar{M}^P$ for all other j and $h_i = h$.

Solution: it can be shown that $M_0 = (m+1)(2m+1)Fh/6$ and $2\sum_{j=1}^{n}\sum_{i=1}^{m}\bar{M}^P_{i,j} = 2mn\bar{M}^P$, i.e., $F = 12mn\bar{M}^P/(m+1)(2m+1)h$. Similarly, Eq. (23) reduces to $\frac{Fh(m+1)}{2} = \frac{n\bar{M}^P}{2} + n\lambda\bar{M}^P + M^P_w$. Equating the last two equations for F, gives after rearrangement:

$$M^P_w > \left[\frac{6m-(1+\lambda)(2m+1)}{(2m+1)}\right]n\bar{M}^P. \tag{39}$$

Appendix 2: example 2, a typical MFUR

Consider the performance of the MFUR of Fig. 7b subjected to forces Fi/m with the following member properties: $I_{m,j} = I_m = I$, $J_{m,j} = 2.4I$ except for $J_{m,0} = J_{m,n} = J = 1.2I$. $M^P_{m,j} = M^P$, $N^P_{m,j} > 2M^P$ and $N^P_{m,0} = N^P_{m,5} > M^P$ for all other j. Assume $P_{i,j} = 0$, $K_{D,i} = \bar{K}_{D,i} = K_B = K_C = 0$. Following Eqs. (33) and (34) the corresponding subframe stiffnesses K_i and moments M^P_i can be computed as shown in Fig. 7a. The MFUR failure load can be computed as$F^P = 20.00M^P/h$.

The roof displacement and the uniform drift can now be estimated as $\Delta_{\mathrm{MFUR}} = \phi_{\mathrm{MFUR}}6\ h = 6F/K$ and $\phi_{\mathrm{MFUR}} = F/Kh$, respectively. The complete elastoplastic solution to this frame can be found in Grigorian and Grigorian (2012). In addition this example can be used to assess the efficiency of the other extreme scenario where $S_i = F_i$.

Appendix 3: example 3, a typical MFUS

The MFUS of Fig. 7c is similar to the MFUR of Example 2. Following Eq. (32), the static equilibrium of the wall gives $Q_{r,m}H = M_{r.0} = 13.8F_rh$ and $Q_{r,m} = 13.8F_rh/6h = 2.3F_r$. Since the uniform drift rule, Eq. (33), can be simplified as $K_{r,i} = (h_m/h_i)K_{u,r,m} = K_u$, the uniform drift and the maximum roof level displacement can be estimated as $\phi_{\mathrm{MFUS}} = Q/K_uh$ and $\Delta_{\mathrm{MFUS}} = \phi_{MFUS}6\ h = 6Q/K_u$, respectively. The MFUS plastic failure load can be shown to be equal to $F^P = 120.00M^P/13.8\ h$. In order to compare the two systems, K_u should be selected in such a way that $\Delta_{\mathrm{MFUS}} = \Delta_{\mathrm{MFUR}}$. This gives $K_u = 2.3K$ for this particular example and leads to the general formula:

$$K_{u,m} = \frac{M_0}{F_mh_m}K_m. \tag{40}$$

Next assuming that the unit weight of any subframe can be related to its plastic strength through a constant of proportionality, γ, then the total weights of the MFUS and MFUR may be computed as

$$G_{\mathrm{MFUS}} = \gamma[2M^P_u + 2\times 1.25M^P_u + 1.5M^P_u] = 6\gamma M^P_u = 0.69\gamma Fh, \tag{41}$$

$$G_{\mathrm{MFUR}} = \gamma[M^P + 1.8M^P + 3M^P + 3.5M^P + 4.5M^P] = 0.69\gamma M^P. \tag{42}$$

In conclusion, an MFUS is as weight efficient as an equivalent MFUR and that MFUS-RRW combinations can perform more efficiently under both linear as well as non-linear loading states, than their non conforming counterparts.

References

AISC/SEAOC (2001) Recommended provisions for buckling-restrained braced frames. American Institute of Steel Construction/Structural Engineers Association of California, Chicago

Ajrab J, Pekcan G, Mander J (2004) Rocking wall-frame structures with supplemental tendon systems. J Struct Eng 130(6):895–903

ASCE (2007) Seismic rehabilitation of existing buildings, ASCE/SEI Standard 41-06 with supplement 1. American Society of Civil Engineers, Reston

Aslam M, Goddon WG, Scalise DT (1980) Earthquake rocking response of rigid bodies. J Struct Div ASCE 106(2):377–392

Chancellor NB, Eatherton MR, Roke DA, Akbas T (2014) Self-centering seismic force resisting systems: high performance structures for the city of tomorrow. Buildings 4:520–548

Christopoulos C, Filiatrault A, Uang CM, Folz B (2002) Post-tensioned energy dissipating connections for moment-resist J. H.

(2011). Seismic design and shake table tests of a steel post-tensioned self-centering moment frame with a slab accommodating frame expansion. Earthq Eng Struct Dyn 40(11):1241–1261

Deierlein GG, Ma X, Eatherton M et al. (2009) Collaborative research on development of innovative steel braced frame systems with controlled rocking and replaceable fuses. In: Proceedings of 6th international conference on urban earthquake engineering, Tokyo, pp 413–416

Deierlien GG, Reinhorn AM, Willford MR (2010) Nonlinear structural analysis for seismic design. NEHRP Seismic Design Technical Brief No.4, Gaithersburg, MD, NIST GCR 10-917-5

Dowden DM, Bruneau M (2011) New Z-BREAKSS: post-tensioned rocking connection detail free of beam growth. AISC Eng J 48:153–158

Eatherton ER, Ma X, Krawinkler H, Mar H, Billington S, Hajjar JF, Deierlein G (2014) Design concepts for controlled rocking of self-centering steel-braced frames. J Struct Div ASCE. doi:10.1061/(ASCE)ST.1943-541X.0001047

Englekirk RE (2002) Design-Construction of the paramount-a 39-story precast prestressed concrete building. PCI J 47:56–71

FEMA (2005) Improvement of nonlinear static seismic analysis procedures: FEMA report 440, Washington, DC, USA

FEMA (2006) Next-generation performance based seismic design guidelines program plan for new and existing buildings. FEMA report 445, Washington, DC, USA

FEMA (2009) Quantification of building seismic performance factors, FEMA report 695, Washington, DC, USA

Garlock M, Sause R, Ricles JM (2007) Behavior and design of post-tensioned steel frame systems. J Struct Eng ASCE 133(3):389–399

Grigorian M, Grigorian C (2011) Performance control for seismic design of moment frames. J Constr Steel Res 67:1106–1114

Grigorian M, Grigorian C (2012) Performance control: a new elastic-plastic design procedure for earthquake resisting moment frames. J Struct Div ASCE 6(138):473–483

Grigorian M, Grigorian C (2015) An Introduction to the structural design of rocking wall-frames with a view to collapse prevention, self alignment and repairability. Struct Design Tall Spec Build. doi:10.1002/tal.1230

Grigorian C, Grigorian M (2016) Performance control and efficient design of rocking-wall moment-frames. J Struct Div ASCE 2(142):473–483. doi:10.1061/(ASCE)ST.1943-541X.0001411)

Grigorian M, Moghadam AS, Mohammadi H (2017) On rocking core-moment frame design. In: 16th world conference on earthquake engineering, 16WCEE, Chile, Paper No. 397

Hajjar JF, Sesen AH, Jampole E, Wetherbee A (2013) A synopsis of sustainable structural systems with rocking, self-centering, and articulated energy-dissipating fuse. Department of Civil and Environmental Engineering Reports, NEU-CEE-2013-01, Northeastern University, Boston, Massachusetts, USA

Hamburger RO, Krawinkler H, Malley JO, Adan SM (2007) Seismic design of steel special moment frames: a guide for practicing engineers. NEHRP; seismic design technical brief, No. 2, USA

Janhunen B, Tipping S, Wolfe J, Mar D (2012) Seismic retrofit of a 1960s steel moment- frame high-rise using pivoting spine. In: Proceedings of the 2012 annual meeting of the Los Angeles tall buildings structural design council

MacRae GA (2011) The continuous column concept-development and use.In: Proceedings of the ninth Pacific conference on earthquake engineering building an earthquake-resilient society, 14–16 April, Auckland, NZ

MacRae GA, Kawashima K (1997) Post-earthquake residual displacements of bilinear oscillators. Earthq Eng Struct Dynam 26(7):701–716

MacRae GA, Kimura Y, Roeder C (2004) Effect of column stiffness on braced frame seismic behavior. J Struct Div ASCE 130(3):381–391

Panian L, Steyer M, Tipping S (2007) An innovative approach to earthquake safety and concrete construction. J Post Tens Inst 5(1):7–16

Seymour D, Laflamme S (2011) Quasi-Static analysis of rocking wall systems. Department of Civil and Environmental Engineering, Massachusetts Institute of Technology, Cambridge

Wada A, Connor JJ, Kawai H, Iwata M, Watanabe A (1992) Damage tolerant structures. In: Fifth USA–Japan workshop on the improvement of building structural design and construction practices 1–12, USA

Wada A, Qu Z, Ito H, Motoyui S, Sakata H, Kasai K (2012) Pin supported walls for enhancing the seismic behavior of building structures. Earthq Eng Struct Dyn 41:2075–2092

Zibaei H, Mokari J (2014) Evaluation of seismic behavior improvement in RC MRFs retrofitted by controlled rocking wall systems. Struct Design Tall Spec Build 23:995–1006